CHEMISTRY OF MATERIALS
Article

Chem. Mater. **2009,** *21,* 4155–4162 4155
DOI:10.1021/cm900228c

Interlayer surface modification of the protonated ion-exchangeable layered perovskite $HLaNb_2O_7 \cdot xH_2O$ with organophosphonic acids

Akira Shimada,[†] Yoriyoshi Yoneyama,[†] Seiichi Tahara,[†] P. Hubert Mutin,[‡] and Yoshiyuki Sugahara*,[†]

[†]*Department of Applied Chemistry, Waseda University, Okubo-3, Shinjuku-ku, Tokyo 169-8555, Japan, and* [‡]*Institut Charles Gerhardt, UMR 5253 CNRS-UM2-ENSCM-UM1, Université Montpellier 2, Place Eugène Bataillon, 34095 Montpellier Cedex 5, France*

Received January 24, 2009. Revised Manuscript Received July 1, 2009

The interlayer surface of a protonated form of the Dion−Jacobson-type ion-exchangeable layered perovskite, $HLaNb_2O_7 \cdot xH_2O$ (HLaNb), has been successfully modified with various organophosphonic acids [phenylphosphonic acid ($PhPO(OH)_2$, PPA) and *n*-alkylphosphonic acids (n-C_nH_{2n+1}-$PO(OH)_2$ with $n = 4-18$, APAs)] to produce graft-type organic derivatives using an *n*-decoxy derivative of HLaNb (C_{10}O-HLaNb) as an intermediate. The interlayer distances of the products are changed from that of the intermediate, 2.73 nm, to 2.31 (PPA/C_{10}O-HLaNb) and 2.31−5.26 (APAs/C_{10}O-HLaNb) nm. IR and solid-state ^{13}C CP/MAS NMR spectra of the products reveal that *n*-decoxy groups are removed and phenyl (PPA/C_{10}O-HLaNb) or *n*-alkyl groups (APA/C_{10}O-HLaNb) are introduced. Elemental analysis reveals that the amounts of PPA- and APA-moieties are 0.88−0.99 per $[LaNb_2O_7]$, corresponding approximately to the amount of the *n*-decoxy groups in C_{10}O-HLaNb. The environment of interlayer species in PPA/C_{10}O-HLaNb is assumed to be monodentate PhPO(OH)(ONb) based on the IR results (the P−O stretching and P−OH stretching bands at ∼1030 and ∼950 cm^{-1}) and the reaction between PPA/C_{10}O-HLaNb and *n*-butylamine ($-NH_2$/POH = 1.0). Scanning electron micrographs of the products reveal that the morphology is clearly preserved during the reactions with PPA or APAs, indicating that they are graft-type rather than dissolution−recrystallization-type reactions. Because water is required for the reaction between PPA and C_{10}O-HLaNb, this reaction is assumed to proceed via the formation of an $(HO)NbO_5$ site and its subsequent reaction with PPA. A linear relationship is clearly observed between the number of carbon atoms in the *n*-alkyl chains and the interlayer distances of APAs/C_{10}O-HLaNb, and a structural model of APAs/C_{10}O-HLaNb with a *n*-alkyl chain tilt angle of 57° is proposed.

Introduction

Surface modification of metal oxide particles with organic molecules has been widely studied as a method of preparing inorganic−organic hybrid materials that are utilizable for various applications, including separation and catalysis.[1,2] The most common modification method is silylation, in which organosilanes such as organochlorosilanes and organoalkoxysilanes are generally employed for the modification of oxide particles, especially silica particles.[3] Modification with organophosphorus compounds has also been developed,[4−6] and metal−oxygen−phosphorus (M−O−P) bonds can be formed on many metal oxides, including ZrO_2,[7] TiO_2,[8−10] Nb_2O_5,[11] Ta_2O_5,[11] SnO_2,[12] Al_2O_3,[13] SiO_2,[14,15] and SiO_2-TiO_2[16] using organophosphorus compounds bearing POH groups, such as organophosphonic acids and organophosphinic acids. The major advantages of this type of modification include the high stability of M−O−P bonds, lack of condensation between two POH groups (to form P−O−P bonds), and possible use of water as a solvent; insensitivity to water is particularly advantageous, because the homocondensation

*Corresponding author. Fax. 81-3-5286-3204. E-mail: ys6546@waseda.jp.

(1) Neouze, M.-A.; Schubert, U. *Monatsh. Chem.* **2008**, *139*, 183–195.
(2) Nawrocki, J. *J. Chromatogr., A* **1997**, *779*, 29–71.
(3) Van Der Voort, P.; Vansant, E. F. *J. Liq. Chromatogr. Relat. Technol.* **1996**, *19*, 2723–2752.
(4) Mutin, P. H.; Guerrero, G.; Vioux, A. *C. R. Chim.* **2003**, *6*, 1153–1164.
(5) Vioux, A.; Le Bideau, J.; Mutin, P. H.; Leclercq, D. *Top. Curr. Chem.* **2004**, *232*, 145–174.
(6) Mutin, P. H.; Guerrero, G.; Vioux, A. *J. Mater. Chem.* **2005**, *15*, 3761–3768.
(7) Gao, W.; Dickinson, L.; Grozinger, C.; Morin, F. G.; Reven, L. *Langmuir* **1996**, *12*, 6429–6435.
(8) Guerrero, G.; Mutin, P. H.; Vioux, A. *Chem. Mater.* **2001**, *13*, 4367–4373.
(9) Lafond, V.; Gervais, C.; Maquet, J.; Prochnow, D.; Babonneau, F.; Mutin, P. H. *Chem. Mater.* **2003**, *15*, 4098–4103.
(10) Brodard-Severac, F.; Guerrero, G.; Maquet, J.; Florian, P.; Gervais, C.; Mutin, P. H. *Chem. Mater.* **2008**, *20*, 5191–5196.
(11) Hofer, R.; Textor, M.; Spencer, N. D. *Langmuir* **2001**, *17*, 4014–4020.
(12) Holland, G. P.; Sharma, R.; Agola, J. O.; Amin, S.; Solomon, V. C.; Singh, P.; Buttry, D. A.; Yarger, J. L. *Chem. Mater.* **2007**, *19*, 2519–2526.
(13) Guerrero, G.; Mutin, P. H.; Vioux, A. *J. Mater. Chem.* **2001**, *11*, 3161–3165.
(14) Lukes, I.; Borbaruah, M.; Quin, L. D. *J. Am. Chem. Soc.* **1994**, *116*, 1737–1741.
(15) Blümel, J. *Inorg. Chem.* **1994**, *33*, 5050–5056.
(16) Mutin, P. H.; Lafond, V.; Popa, A. F.; Granier, M.; Markey, L.; Dereux, A. *Chem. Mater.* **2004**, *16*, 5670–5675.

Published on Web 08/27/2009

of the silylation reagent is a major concern for surface modification by silylation.

Surface modification can also be applied to some layered compounds to produce organically modified interlayer surfaces where organic groups are arranged ideally in an ordered manner. Because the first example of the silylation of crystalline silicic acid, magadiite,[17] was reported, various layered compounds, such as other crystalline silicic acids[18,19] and layered titanate[20] have been employed. To date, this type of modification has been used to develop graft-type organic derivatives, such as adsorbents with selective adsorption behavior,[21,22] porous materials,[23] and new layered silica nanosheets with hydrolyzable alkoxysilyl groups.[24] As concerns interlayer surface modification with organophosphonic acids [$RPO(OH)_2$] or related compounds, $(HO)_2OP$-R-$PO(OH)_2$, intercalation of anionic guest species was first achieved via anion-exchange reactions or reactions of molten phenylphosphonic acid with layered double hydroxides (LDHs) or its calcined product, and subsequent heat-treatments of the anion-intercalated compounds led to the formation of graft-type organic derivatives.[25−28] Interlayer surface modification of 1:1 type silicate minerals, kaolinite and halloysite, with phenylphosphonic acid was also attempted,[29,30] but it was clarified that the final layered structures were obtained via dissolution and a subsequent recrystallization process because of the acidity of phenylphosphonic acid.[31] The reactions of other silicates, phlogopite and chrysotile, with phenylphosphonic acid also involved partial dissolution of the silicate layers (leaching process).[32,33] Organic derivatization of bayerite[34] and edge derivatization of exfoliated α-$Zr(HPO_4)_2 \cdot H_2O$ nanosheets[35] were also achieved using organophosphonic acids.

Ion-exchangeable layered perovskites consist of perovskite-like slabs [$A_{n-1}B_nO_{3n+1}$] and interlayer cations, M. Ion-exchangeable layered perovskites can be classified into two families, Dion-Jacobson phases ($M[A_{n-1}B_nO_{3n+1}]$) and Ruddlesden−Popper phases ($M_2[A_{n-1}B_nO_{3n+1}]$).[36] Acid treatments of the ion-exchangeable layered perovskites leads to the formation of protonated forms, $H_x[A_{n-1}B_nO_{3n+1}]$, ($x = 1, 2$). A few protonated forms of both the Dion-Jacobson phases ($HLaNb_2O_7 \cdot xH_2O$, $HCa_2Nb_3O_{10} \cdot xH_2O$) and the Ruddlesden−Popper phase ($H_2La_2Ti_3O_{10}$) can be modified with alcohols and trifluoroacetic acid to form surface alkoxy and trifluoroacetate groups.[37−43] It is also possible to modify interlayer surface of Dion-Jacobson-type $HCa_2Nb_3O_{10} \cdot xH_2O$ by using silylation reagents possessing trimethoxysilyl groups.[44−47]

We report here the modification of the interlayer surface of an ion-exchangeable layered perovskite, $HLaNb_2O_7 \cdot xH_2O$ (HLaNb), with various organophosphonic acids, $RPO(OH)_2$, where R refers to phenyl groups [phenylphosphonic acid (PPA)] or *n*-alkyl groups (*n*-C_nH_{2n+1} groups with $n = 4-18$) [*n*-alkylphosphonic acids (APAs)] (see Scheme 1). An *n*-decoxy derivative of HLaNb ($C_{10}O$-HLaNb) was used as an intermediate. Structural and spectroscopic characterization is presented, and a reaction mechanism and structural models of the interlayer space are discussed.

Experimental Section

Instrumentation. X-ray diffraction (XRD) patterns were obtained with a Rigaku RINT-1100 diffractometer (Mn-filtered FeKα radiation). Infrared (IR) spectra were recorded on a JASCO FT/IR-460 Plus spectrometer using the KBr method. Solid-state ^{13}C and ^{31}P nuclear magnetic resonance (NMR) spectroscopy was performed with a JEOL CMX-400 (9.4 T) spectrometer at 100.54 and 161.84 MHz, respectively. Solid-state ^{13}C NMR spectra were obtained with cross-polarization (CP) and magic angle spinning (MAS) techniques (pulse delay, 5s; contact time, 1.5 s; spinning rate, 8 kHz), while solid-state ^{31}P NMR spectra were obtained with a MAS technique only (pulse delay, 20 s; pulse angle, 90°; spinning rate, 8 kHz). Inductively coupled plasma emission spectrometry was performed with a Thermo Jarrel Ash ICAP-574 II instrument after dissolving the sample (about 1.8 mg) in a mixture of 5 mL of conc. HNO_3 (69−70 mass%), 5 mL of conc. H_2SO_4 (> 96 mass%), and 10 mL

(17) Ruiz-Hitzky, E.; Rojo, J. M. *Nature* **1980**, *287*, 28–30.
(18) Yanagisawa, T.; Kuroda, K.; Kato, C. *Bull. Chem. Soc. Jpn.* **1988**, *61*, 3743–3745.
(19) Mochizuki, D.; Shimojima, A.; Kuroda, K. *J. Am. Chem. Soc.* **2002**, *124*, 12082–12083.
(20) (a) Ide, Y.; Ogawa, M. *Angew. Chem. Int. Ed.* **2007**, *46*, 8449–8451. (b) Ide, Y.; Ogawa, M. *Chem. Commun.* **2003**, *9*, 1262–1263.
(21) Ogawa, M.; Okutomo, S.; Kuroda, K. *J. Am. Chem. Soc.* **1998**, *120*, 7361–7362.
(22) Fujita, I.; Kuroda, K.; Ogawa, M. *Chem. Mater.* **2005**, *17*, 3717–3722.
(23) Mochizuki, D.; Kowata, S.; Kuroda, K. *Chem. Mater.* **2006**, *18*, 5223–5229.
(24) Mochizuki, D.; Shimojima, A.; Imagawa, T.; Kuroda, K. *J. Am. Chem. Soc.* **2005**, *127*, 7183–7191.
(25) Wang, J. D.; Serrette, G.; Tian, Y.; Clearfield, A. *Appl. Clay Sci.* **1995**, *10*, 103–115.
(26) Carlino, S.; Hudson, M. J.; Husain, S. W.; Knowles, J. A. *Solid State Ionics* **1996**, *84*, 117–129.
(27) Costantino, U.; Casciola, M.; Massinelli, L.; Nocchetti, M.; Vivani, R. *Solid State Ionics* **1997**, *97*, 203–212.
(28) Prévot, V.; Forano, C.; Besse, J. P. *Appl. Clay Sci.* **2001**, *18*, 3–15.
(29) Guimarães, J. L.; Peralta-Zamora, P.; Wypych, F. *J. Colloid Interface Sci.* **1998**, *206*, 281–287.
(30) Breen, C.; D'Mello, N.; Yarwood, J. *J. Mater. Chem.* **2002**, *12*, 273–282.
(31) Gardolinski, J. E. F. C.; Lagaly, G.; Czank, M. *Clay Minerals* **2004**, *39*, 391–404.
(32) Trobajo, C.; Khainakov, S. A.; Espina, A.; García, J. R.; Salvadó, M. A.; Pertierra, P.; García-Granda, S.; Martín-Izard, A.; Bortun, A. I. *Chem. Mater.* **2001**, *13*, 4457–4462.
(33) Wypych, F.; Schreiner, W. H.; Mattoso, N.; Mosca, D. H.; Marangon, R.; da S. Bento, C. A. *J. Mater. Chem.* **2003**, *13*, 304–307.
(34) Raki, L.; Detellier, C. *Chem. Commun.* **1996**, *1996*, 2475–2476.
(35) Kaschak, D. M.; Johnson, S. A.; Hooks, D. E.; Kim, H.-N.; Ward, M. D.; Mallouk, T. E. *J. Am. Chem. Soc.* **1998**, *120*, 10887–10894.
(36) Schaak, R. E.; Mallouk, T. E. *Chem. Mater.* **2002**, *14*, 1455–1471.
(37) Tahara, S.; Sugahara, Y. *Recent Dev. Inorg. Chem.* **2004**, *4*, 13–34.
(38) Takahashi, S.; Nakato, T.; Hayashi, S.; Sugahara, Y.; Kuroda, K. *Inorg. Chem.* **1995**, *34*, 5065–5069.
(39) Suzuki, H.; Notsu, K.; Takeda, Y.; Sugimoto, W.; Sugahara, Y. *Chem. Mater.* **2003**, *15*, 636–641.
(40) Tahara, S.; Sugahara, Y. *Langmuir* **2003**, *19*, 9473–9478.
(41) Tahara, S.; Ichikawa, T.; Kajiwara, G.; Sugahara, Y. *Chem. Mater.* **2007**, *19*, 2352–2358.
(42) Takeda, Y.; Suzuki, H.; Notsu, K.; Sugimoto, W.; Sugahara, Y. *Mater. Res. Bull.* **2006**, *41*, 834–841.
(43) Takeda, Y.; Momma, T.; Osaka, T.; Kuroda, K.; Sugahara, Y. *J. Mater. Chem.* **2008**, *18*, 3581–3587.
(44) Kim, J. Y.; Hiramatsu, H.; Osterloh, F. E. *J. Am. Chem. Soc.* **2005**, *127*, 15556–15561.
(45) Kim, J. Y.; Osterloh, F. E.; Hiramatsu, H.; Dumas, R. K.; Liu, K. *J. Phys. Chem. B* **2005**, *109*, 11151–11157.
(46) Kim, J. Y.; Osterloh, F. E. *J. Am. Chem. Soc.* **2006**, *128*, 3868–3869.
(47) Compton, O. C.; Mullet, C. H.; Chiang, S.; Osterloh, F. E. *J. Phys. Chem. C* **2008**, *112*, 6202–6208.

Scheme 1. Overview of the Modification of the Ion-Exchangeable Layered Perovskite HLaNb with Organophosphonic Acids

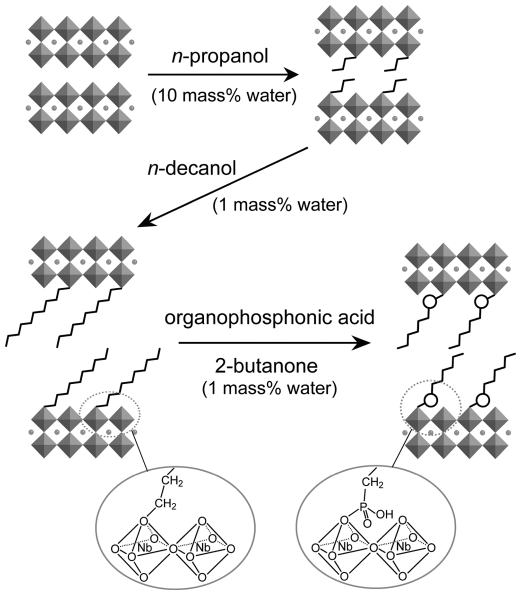

of HF (46−48 mass%) at 200 °C for 2 h. Elemental analysis was performed with a Perkin-Elmer PE2400 II instrument.

Materials. $HLaNb_2O_7 \cdot xH_2O$ (HLaNb) and its *n*-decoxy derivative ($C_{10}O$-HLaNb) were prepared as described elsewhere.[39] Phenylphosphonic acid was employed after purification by recrystallization. *n*-Butylphophonic acid and *n*-hexylphosphonic acid were prepared from *n*-$C_4H_9POCl_2$ and *n*-$C_6H_{13}POCl_2$ via hydrolysis and subsequent recrystallization. Other *n*-alkylphosphonic acids (*n*-octyl, *n*-decyl-, *n*-dodecyl, and *n*-octadecyl-) were prepared from triethyl phosphonate and corresponding 1-bromoalkanes; diethyl *n*-alkylphosphonates were prepared by a Michaelis−Arbuzov reaction and further hydrolyzed with conc. HCl, as described elsewhere.[48]

Interlayer Surface Modification. Typically, 0.1 g of $C_{10}O$-HLaNb, 20 mL of 2-butanone containing 1 mass % of water, and PPA (or APA) were sealed in an ampule with $C_{10}O$-HLaNb: PPA (or APA) = 1:4 in a molar ratio and heated at 80 °C for 48 h (or 72 h for *n*-octadecylphosphonic acid). The crude product was separated by centrifugation and washed with an excess of acetone. The resultant product was analyzed after air-drying or drying at 120 °C. To examine the effect of water, we conducted the reaction between $C_{10}O$-HLaNb and PPA in distilled 2-butanone (with no addition of water) under a nitrogen atmosphere using standard Schlenk techniques[49] to exclude moisture.

Reaction between PPA/$C_{10}O$-HLaNb and *n*-Butylamine. About 0.1 g of the product of the reaction between $C_{10}O$-HLaNb and PPA was sealed with 10 mL of *n*-butylamine and 10 mL of *n*-heptane in an ampule. The ampule was then heated at 70 °C for 24 h. After separation by centrifugation, the crude product was washed once with *n*-heptane and three times with acetone and then air-dried.

Results and Discussion

Reactions between $C_{10}O$-HLaNb and Organophosphonic Acids. Figure 1 shows the XRD patterns of $C_{10}O$-HLaNb and the products of the reactions between $C_{10}O$-HLaNb and various organophosphonic acids (PPA and APAs). In the XRD patterns of all the products, the reflection due to the interlayer distance of $C_{10}O$-HLaNb (d = 2.73 nm) disappears. New corresponding reflections appear in low-angle regions at d = 2.31 nm for the reaction with PPA and at d = 2.31−5.26 nm for the reactions with APAs. The d values observed for the products of the reactions with APAs increase with increases in the length of the *n*-alkyl chain (*n*-butylphosphonic acid, 2.31 nm; *n*-hexylphosphonic acid, 2.73 nm; *n*-octylphosphonic acid, 3.09 nm; *n*-decylphosphonic acid, 3.53 nm; *n*-dodecylphosphonic acid, 3.98 nm; and *n*-octadecylphosphonic acid, 5.26 nm). The interlayer distances for all the reaction products decrease by ~ 0.1 nm upon drying at 120 °C (Table 1). The reflections at 2θ = 28.8 and 41.2°, which are indexed as (100) and (110) for $C_{10}O$-HLaNb and therefore correspond to the ordering of ions in the perovskite-like slab, are observed at the same 2θ angles, indicating that the structure of the perovskite-like slab is retained upon reactions with PPA and APAs.

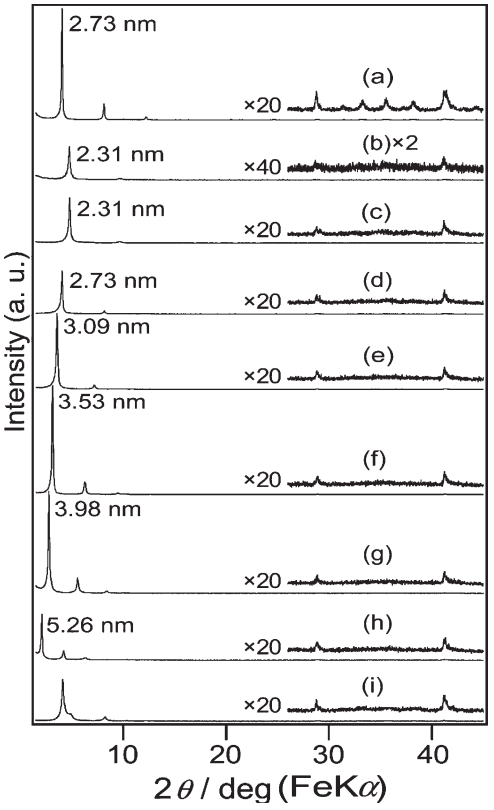

Figure 1. XRD patterns of (a) $C_{10}O$-HLaNb, (b) the product of the reaction between $C_{10}O$-HLaNb and phenylphosphonic acid, (c) the product of the reaction between $C_{10}O$-HLaNb and *n*-butylphosphonic acid, (d) the product of the reaction between $C_{10}O$-HLaNb and *n*-hexylphosphonic acid, (e) the product of the reaction between $C_{10}O$-HLaNb and *n*-octylphosphonic acid, (f) the product of the reaction between $C_{10}O$-HLaNb and *n*-decylphosphonic acid, (g) the product of the reaction between $C_{10}O$-HLaNb and *n*-dodecylphosphonic acid, (h) the product of the reaction between $C_{10}O$-HLaNb and *n*-octadecylphosphonic acid, and (i) the product of the reaction between $C_{10}O$-HLaNb and phenylphosphonic acid under anhydrous conditions.

The organic species were characterized by spectroscopic analyses. The solid-state ^{13}C CP/MAS NMR spectra of the products of the reactions between $C_{10}O$-HLaNb

(48) Bhattacharya, A. K.; Thyagarajan, G. *Chem. Rev.* **1981**, *81*, 415–430.
(49) Shriver, D. F.; Drezdzon, M. A. *The Manipulation of Air-Sensitive Compounds*, 2nd ed.; Wiley-Interscience: New York, 1986.

Table 1. Interlayer Distances of $C_{10}O$-HLaNb and the Products of the Reactions between $C_{10}O$-HLaNb and Organophosphonic Acids before and after Drying at 120°C

		interlayer distance (nm)		
sample name	organophosphonic acid	before drying	after drying	Δ (nm)
$C_{10}O$-HLaNb		2.73		
PPA/$C_{10}O$-HLaNb	phenylphosphonic acid	2.31	2.18	0.13
$C_4PA/C_{10}O$-HLaNb	*n*-butylphosphonic acid	2.31	2.19	0.12
$C_6PA/C_{10}O$-HLaNb	*n*-hexylphosphonic acid	2.73	2.63	0.10
$C_8PA/C_{10}O$-HLaNb	*n*-octylphosphonic acid	3.09	2.97	0.12
$C_{10}PA/C_{10}O$-HLaNb	*n*-decylphosphonic acid	3.53	3.43	0.10
$C_{12}PA/C_{10}O$-HLaNb	*n*-dodecylphosphonic acid	3.98	3.88	0.10
$C_{18}PA/C_{10}O$-HLaNb	*n*-octadecylphosphonic acid	5.26	5.16	0.10

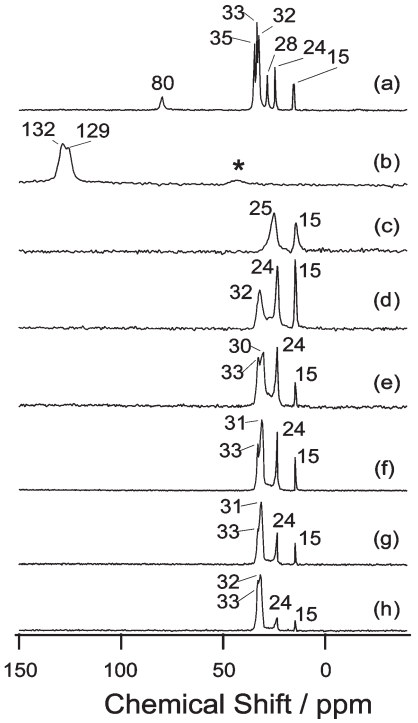

Figure 2. Solid-state ^{13}C CP/MAS NMR spectra of (a) $C_{10}O$-HLaNb, (b) the product of the reaction between $C_{10}O$-HLaNb and phenylphosphonic acid, (c) the product of the reaction between $C_{10}O$-HLaNb and *n*-butylphosphonic acid, (d) the product of the reaction between $C_{10}O$-HLaNb and *n*-hexylphosphonic acid, (e) the product of the reaction between $C_{10}O$-HLaNb and *n*-octylphosphonic acid, (f) the product of the reaction between $C_{10}O$-HLaNb and *n*-decylphosphonic acid, (g) the product of the reaction between $C_{10}O$-HLaNb and *n*-dodecylphosphonic acid, and (h) the product of the reaction between $C_{10}O$-HLaNb and *n*-octadecylphosphonic acid. Spinning sidebands are marked with asterisks.

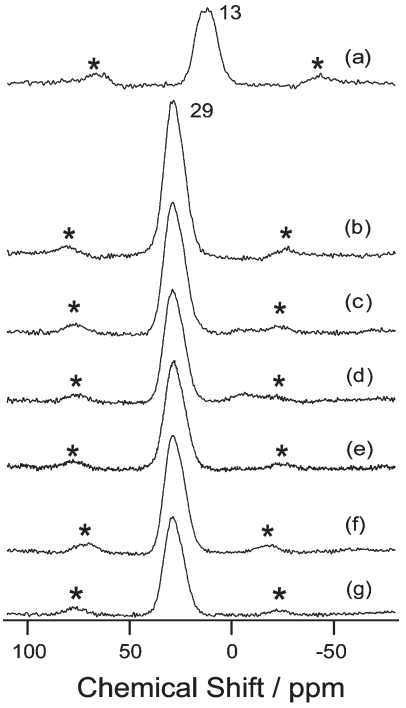

Figure 3. Solid-state ^{31}P MAS NMR spectra of (a) the product of the reaction between $C_{10}O$-HLaNb and phenylphosphonic acid, (b) the product of the reaction between $C_{10}O$-HLaNb and *n*-butylphosphonic acid, (c) the product of the reaction between $C_{10}O$-HLaNb and *n*-hexylphosphonic acid, (d) the product of the reaction between $C_{10}O$-HLaNb and *n*-octylphosphonic acid, (e) the product of the reaction between $C_{10}O$-HLaNb and *n*-decylphosphonic acid, (f) the product of the reaction between $C_{10}O$-HLaNb and *n*-dodecylphosphonic acid, and (g) the product of the reaction between $C_{10}O$-HLaNb and *n*-octadecylphosphonic acid. Spinning sidebands are marked with asterisks.

and various organophosphonic acids (PPA and APAs) are demonstrated in Figure 2. In the spectra of all the products, the signal due to the α carbon atom of the *n*-decoxy groups at 80 ppm[39] disappears, indicating that the *n*-decoxy groups are released upon reactions. In the spectrum of the product of the reaction between $C_{10}O$-HLaNb and PPA (PPA/$C_{10}O$-HLaNb), broad signals which are assignable to the phenyl groups[50] are observed at 129 and 132 ppm. In the spectra of the products of the reactions between $C_{10}O$-HLaNb and APAs (APA/$C_{10}O$-HLaNb), signals assignable to the *n*-alkyl groups[7,51] are clearly observed in the range from 15 to 33 ppm. Because the *n*-decoxy groups are released, the observed signals can be assigned to the *n*-alkyl groups in APA moieties.

Figure 3 exhibits the solid-state ^{31}P MAS NMR spectra of the products of the reactions between $C_{10}O$-HLaNb and various organophosphonic acids (PPA and APAs). In the spectrum of PPA/$C_{10}O$-HLaNb, a broad signal is observed at 13 ppm, whereas broad signals are present at 28−30 ppm in the spectra of APA/$C_{10}O$-HLaNb. The solid-state ^{31}P MAS NMR spectra of PPA and APA molecules were also measured. The spectrum of PPA displayed a signal at 22 ppm. In the spectra of APAs with short *n*-alkyl chains (*n*-butylphosphonic acid, *n*-hexylphosphonic acid, *n*-octylphosphonic acid, and *n*-decylphosphonic acid) signals were displayed at 38−39 ppm,

(50) Gervais, C.; Profeta, M.; Lafond, V.; Bonhomme, C.; Azaïs, T.; Mutin, P. H.; Pickard, C. J.; Mauri, F.; Babonneau, F. *Magn. Reson. Chem.* **2004**, *42*, 445–452.
(51) Carter, V. J.; Wright, P. A.; Gale, J. D.; Morris, R. E.; Sastre, E.; Perez-Pariente, J. *J. Mater. Chem.* **1997**, *7*, 2287–2292.

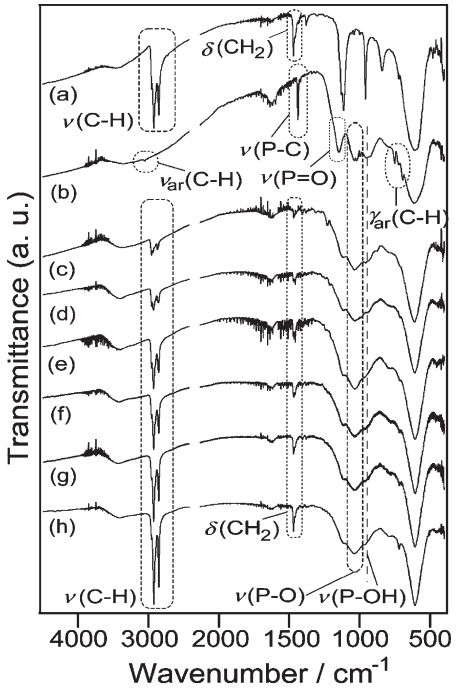

Figure 4. IR spectra of (a) C_{10}O-HLaNb, (b) the product of the reaction between C_{10}O-HLaNb and phenylphosphonic acid, (c) the product of the reaction between C_{10}O-HLaNb and *n*-butylphosphonic acid, (d) the product of the reaction between C_{10}O-HLaNb and *n*-hexylphosphonic acid, (e) the product of the reaction between C_{10}O-HLaNb and *n*-octylphosphonic acid, (f) the product of the reaction between C_{10}O-HLaNb and *n*-decylphosphonic acid, (g) the product of the reaction between C_{10}O-HLaNb and *n*-dodecylphosphonic acid, and (h) the product of the reaction between C_{10}O-HLaNb and *n*-octadecylphosphonic acid.

whereas the solid-state ^{31}P MAS NMR spectra of *n*-dodecylphosphonic acid and *n*-octadecylphosphonic acid showed signals at 31 and 33 ppm, respectively. Thus, the ^{31}P NMR signals of all the products (PPA/C_{10}O-HLaNb and APA/C_{10}O-HLaNb) are shifted upfield (2−11 ppm) from the signals of the corresponding organophosphonic acids (PPA and APAs) in the solid-state ^{31}P MAS NMR spectra.

Figure 4 shows the IR spectra of the products of the reactions between C_{10}O-HLaNb and various organophosphonic acids (PPA and APAs). In the spectra of all the products, the P−O and P−OH stretching bands are present at ∼1030 and ∼950 cm^{-1}, respectively.[8] In addition, in the spectrum of PPA/C_{10}O-HLaNb, adsorption bands assignable to the PPA moieties are also observed: the stretching band of the aromatic C−H group (3050 cm^{-1}); the P−C stretching band characteristic of the P−C_6H_5 group (1440 cm^{-1}); and the C−H out-of-plane deformation bands of the monosubstituted benzene ring (753 and 691 cm^{-1}).[8,52,53] In a similar fashion, adsorption bands due to the APA moieties are present at 2960−2850 (C−H stretching bands) and 1468 (CH_2 bending band) cm^{-1} in all the spectra of APA/C_{10}O-HLaNb.[54,55] The P═O stretching bands, which were present at 1220 and 1230 cm^{-1} in the spectra of PPA and APAs (not shown), respectively, are not detected at corresponding positions in any of the spectra of the reaction products. The lack of P═O stretching bands was reported for organophosphonic acid moieties (tridentate[8,56] and monodentate[55] environments) grafted on the surfaces of metal oxide particles. It should also be noted that P═O stretching bands are known to have a relatively large range.[7] Actually, the wavenumbers of the P═O stretching bands depended strongly on the nature of X in $PhPO(OX)_2$ ($PhPO(OH)_2$, 1220 cm^{-1}; $PhPO(OMe)_2$, 1253 cm^{-1}; and $PhPO(OK)_2$, 1162 cm^{-1}). Thus, we could not exclude the possibility that the P═O stretching bands are overlapping with the P−O stretching bands which have shoulders at higher wavenumbers. In addition, it should be noted that the C−H asymmetric and symmetric stretching bands in the spectrum of the product of the reaction between C_{10}O-HLaNb and *n*-$C_{18}H_{37}PO(OH)_2$ (C_{18}PA/C_{10}O-HLaNb) are present at 2849 and 2918 cm^{-1}, respectively, and their positions clearly indicate that the *n*-alkyl chain in C_{18}PA/C_{10}O-HLaNb exhibits an all-trans conformation.[57]

Table 2. Molar Ratios of Nb, La, and P in HLaNb and the Products of the Reactions between C_{10}O-HLaNb and Organophosphonic Acids

sample name	Nb[a]	La	P
HLaNb	2	1.00	
PPA/C_{10}O-HLaNb	2	1.01	0.88
C_4PA/C_{10}O-HLaNb	2	1.00	0.91
C_6PA/C_{10}O-HLaNb	2	1.01	0.92
C_8PA/C_{10}O-HLaNb	2	1.00	0.93
C_{10}PA/C_{10}O-HLaNb	2	1.00	0.94
C_{12}PA/C_{10}O-HLaNb	2	1.00	0.93
C_{18}PA/C_{10}O-HLaNb	2	1.00	0.99

[a] Set to 2.

The molar ratios of Nb, La, and P in the products of the reactions between C_{10}O-HLaNb and various organophosphonic acids (PPA and APAs) derived from phosphorus and metal contents are given in Table 2. The amounts of PPA and APAs moieties calculated from the phosphorus contents are 0.88−0.99 per [$LaNb_2O_7$], values close to the amount of the *n*-decoxy groups (0.88 per [$LaNb_2O_7$]) . In addition, the La/Nb ratio is maintained at 0.5 during the reactions, suggesting the preservation of perovskite-like slabs upon treatments with PPA and APAs.

The morphology of C_{10}O-HLaNb is essentially unchanged upon the reaction with PPA (Figure 5), as is to be expected for true graft-type reactions. The shapes of the particles are plate-like in the scanning electron micrographs of C_{10}O-HLaNb and PPA/C_{10}O-HLaNb, and their particle sizes are very similar. Similar morphology is also observed for all of APAs/C_{10}O-HLaNb (see Figure S1 in the Supporting Information).

(52) Nijs, H.; Clearfield, A.; Vansant, E. F. *Microporous Mesoporous Mater.* **1998**, *23*, 97–108.
(53) Shurvell, H. F., Spectra-Structure Correlations in the Mid- and Far-Infrared. In *Handbook of Vibrational Spectroscopy*; Chalmers, J. M.; Griffiths, P. R., Eds.; John Wiley & Sons: Chichester, U.K., 2002; Vol. *3* Sample Characterization and Spectral Data Processing, p 1783−1816.
(54) Cao, G.; Lee, H.; Lynch, V. M.; Mallouk, T. E. *Solid State Ionics* **1988**, *26*, 63–69.
(55) Schulmeyer, T.; Paniagua, S. A.; Veneman, P. A.; Jones, S. C.; Hotchkiss, P. J.; Mudalige, A.; Pemberton, J. E.; Marder, S. R.; Armstrong, N. R. *J. Mater. Chem.* **2007**, *17*, 4563–4570.
(56) Randon, J.; Blanc, P.; Paterson, R. *J. Membr. Sci.* **1995**, *98*, 119–129.
(57) Vaia, R. A.; Teukolsky, R. K.; Giannelis, E. P. *Chem. Mater.* **1994**, *6*, 1017–1022.

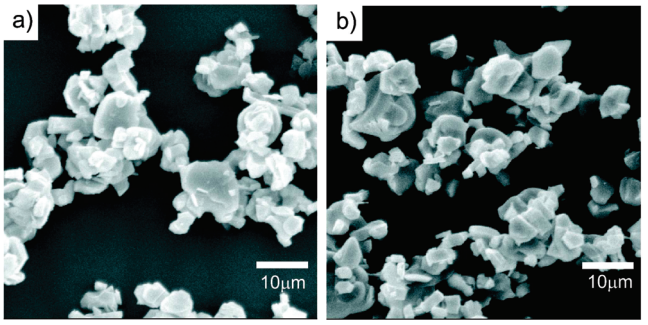

Figure 5. SEM images of (a) C_{10}O-HLaNb and (b) the products of reaction between C_{10}O-HLaNb and phenylphosphonic acid.

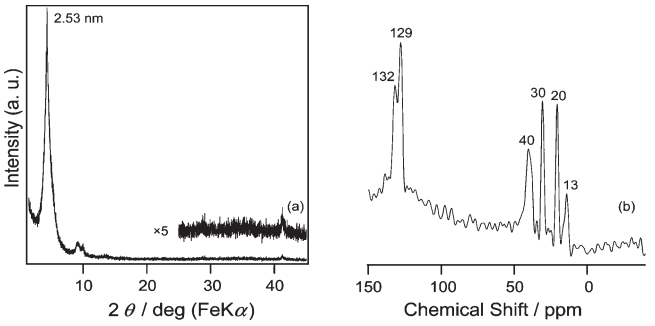

Figure 6. (a) XRD pattern and (b) solid-state ^{13}C CP/MAS NMR spectrum of the product of reaction between PPA/C_{10}O-HLaNb and *n*-butylamine.

Reaction between C_{10}O-HLaNb and PPA under Anhydrous Conditions. Figure 1i shows the XRD pattern of the product of a reaction between C_{10}O-HLaNb and PPA conducted under anhydrous conditions. The profile is essentially the same as that of C_{10}O-HLaNb, with the presence of a weak shoulder reflection at $d \approx 2.26$ nm, the position for PPA/C_{10}O-HLaNb prepared with the addition of water. The IR spectrum of the product (not shown) exhibited very weak adsorption bands due to PPA moieties (3050, 1440, and 1030 cm^{-1}). Thus, a reaction between C_{10}O-HLaNb and PPA is extremely limited under anhydrous conditions.

Reaction between PPA/C_{10}O-HLaNb and *n*-Butylamine. The reactivity of PPA/C_{10}O-HLaNb with *n*-butylamine was studied. The XRD pattern of the product of the reaction between PPA/C_{10}O-HLaNb and *n*-butylamine is shown in Figure 6a. The interlayer distance increases from 2.31 (PPA/C_{10}O-HLaNb) to 2.53 nm and the reflections correspond to the ordering of ions in the perovskite-like slabs are present at $2\theta = 28.8$ and 41.2°, suggesting that PPA/C_{10}O-HLaNb can further accommodate *n*-butylamine in the interlayer space. The relative amount of *n*-butylamine was estimated from the phosphorus content (4.75 mass%) and the nitrogen content (1.92 mass%) to be *n*-butylamine/P = 1.0.

The solid-state ^{13}C CP/MAS NMR spectrum of the product of the reaction between PPA/C_{10}O-HLaNb and *n*-butylamine is demonstrated in Figure 6b. In addition to the signals due to the phenyl groups at 128 and 132 ppm, additional signals were detected at 40, 30, 20, and 13 ppm, all of them assignable to *n*-butyl groups. It is generally accepted that the position of the α carbon atom depends on the state of *n*-alkylamines. Because the observed value (40 ppm) is consistent with the value reported for protonated species (*n*-butylammonium), the interaction between PPA/C_{10}O-HLaNb and *n*-butylamine is an acid−base interaction yielding an *n*-butylammonium ion environment.[58,59]

Identification of the Products of Reactions between C_{10}O-HLaNb and Organophosphonic Acids. The XRD patterns show the changes in the interlayer distance after the reactions of C_{10}O-HLaNb with all the organophosphonic acids examined (PPA and APAs). Because the *n*-decoxy groups were removed and the presence of PPA or APA moieties was demonstrated spectroscopically, the observed change in the interlayer distance should be due to the replacement of the *n*-decoxy groups with PAA- or APA-related groups. Organophosphonic acids are relatively strong acids, and it was shown that the organically modified layered structures, obtained by reaction with layered silicates,[31−33] were formed via dissolution [or at least partial dissolution (leaching)]. In the present study, on the contrary, because perovskite-like slabs are resistant to acid (please note that HLaNb was prepared from $RbLaNb_2O_7$ via treatment with a strong acid, 6 M HCl),[39] only graft-type reactions should be involved. Indeed, scanning electron micrographs of the products (Figure 5 and Figure S1 in the Supporting Information) show that the morphology is preserved during reactions with PPA or APAs, confirming that the reactions are truly graft-type. The XRD and compositional analyses indicate the preservation of the perovskite-like slab structure, and are thus consistent with this formation mechanism.

In terms of the phosphorus environment, we have examined PPA/C_{10}O-HLaNb thoroughly. The observed upfield shift of ^{31}P MAS NMR signals for PPA/C_{10}O-HLaNb as compared to that for PPA supports the formation of Nb−O−P linkages.[7,8,10,60] Its IR spectrum clearly shows the presence of POH groups, and the reaction of PPA/C_{10}O-HLaNb with *n*-butylamine indicates that the amount of acidic sites (accessible to *n*-butylamine) corresponds exactly to the amount of PPA moieties. In PPA/C_{10}O-HLaNb, two acidic sites, the (HO)NbO_5 site and the POH site, are present. The possible amount of the (HO)NbO_5 site is much smaller [12% of the (HO)NbO_5 sites initially present in HLaNb], however, and the number of *n*-butylamine reacted corresponds exactly to the number of PPA moieties. Accordingly, we assume that the PPA moieties possess one P−OH group and form one Nb−O−P linkage.

On the basis of the above considerations, two possible PPA-moiety environments, a monodentate PhPO(OH)(ONb) environment and a bidentate PhP(OH)$(ONb)_2$

(58) Atta-Ur-Rahman, T. I., *Nuclear Magnetic Resonance: Basic Principles*; Springer-Verlag: New York, 1986; p 148.
(59) Tahara, S.; Yamashita, T.; Kajiwara, G.; Sugahara, Y. *Chem. Lett.* **2006**, *35*, 1292–1293.
(60) Francisco, M. S. P.; Cardoso, W. S.; Gushikem, Y.; Landers, R.; Kholin, Y. V. *Langmuir* **2004**, *20*, 8707–8714.

environment, can be proposed. As regards the P=O groups, it is not likely that oxygen atoms in the P=O groups coordinate to niobium, a possible Lewis acid site, because a 7-coordinated environment with no change in lattice parameters would be required.[61] Thus, although the presence of the P=O groups is not clearly shown by the IR spectrum of PPA/C_{10}O-HLaNb, it is highly likely that the P=O groups are still present in PPA/C_{10}O-HLaNb, and the surface species should be monodentate PhPO(OH)(ONb). Similar environments, monodentate RPO(OH)(ONb), should also be assumed for APA/C_{10}O-HLaNb.

To examine the stability of the grafted PPA-moiety, we dispersed PPA/C_{10}O-HLaNb in both acidic and basic aqueous solutions. PPA/C_{10}O-HLaNb did not react with an excess of 3 M HCl (at 60 °C for 24 h), in accordance with the expectation based on the use of organophosphonic acids in the preparation procedure. When PPA/C_{10}O-HLaNb was dispersed in an excess amount of 1 M NaOH at room temperature for 24 h, on the contrary, the interlayer distance decreased to 1.34 nm, indicating that hydrolysis occurred. This relatively low stability of the PPA moiety appears to be ascribable to the monodentate PhPO(OH)(ONb) environment.

The overall reaction could thus be expressed as follows

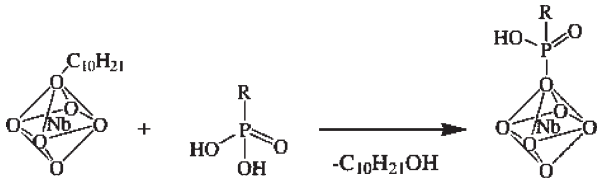

It should be noted that the reaction was very limited when no water was added, indicating that a direct reaction between PPA and the $(C_{10}H_{21}O)NbO_5$ site is not a likely major process. For alcohol-exchange-type reactions of HLaNb, a hydrolysis and subsequent reesterification mechanism was proposed.[39,40] We therefore propose a similar type of reaction in the present system

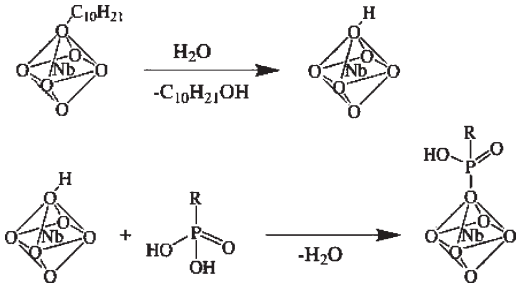

The limited process of the reaction under anhydrous conditions could be due to either the presence of a trace of water or the occurrence of a slow direct reaction between the $(C_{10}H_{21}O)NbO_5$ site and PPA.

When C_{10}O-HLaNb was reacted with phosphonic acid [$HPO(OH)_2$], no reaction was observed, indicating that organic groups in PPA and APAs play an important role in facilitating the insertion of phosphorus compounds into the interlayer space. The use of an *n*-propoxy derivative of HLaNb (d = 1.54 nm) also led to no reaction, suggesting the importance of a large interlayer distance of an intermediate. Thus, it is likely that the hydrolysis proceeds in a very limited manner, so that both the $(C_{10}H_{21}O)NbO_5$ sites (maintaining a large interlayer distance) and the $(OH)NbO_5$ sites are present in the same interlayer space.

Arrangement of Organic Groups in the Interlayer Space. The arrangement of PPA and APA moieties can be discussed on the basis of the cross-section area of the $-PO(O^-)_2$ group, 0.24 nm,[2,62] which corresponds to the area of a circle with a diameter of 0.49 nm. In HLaNb, every other apical oxygen atom possesses a proton (corresponding to one proton per $[LaNb_2O_7]$ bearing two apical oxygen atoms on both sides of the slab), and the distance between two reactive sites $[(HO)NbO_5]$ is 0.550 nm ($= \sqrt{2}a$).[61] When all the $(HO)NbO_5$ sites could be occupied by PPA moieties, the amount of PPA is maximal, 1.0 per $[LaNb_2O_7]$. Thus, the observed amounts of PPA and APA moieties (0.88−0.99 per $[LaNb_2O_7]$) are well-consistent with the proposed models in terms of lateral dimension.

The interlayer distance in PPA/C_{10}O-HLaNb (after drying) is 2.18 nm. Because the thickness of the perovskite-like slab ($[LaNb_2O_7]$) is estimated to be the sum of $2a$ (0.778 nm) and twice the ionic radius of an oxygen ion (0.132 nm), that is, 1.042 nm, the gallery height is estimated to be 1.14 nm. Because the size of PPA is about 0.63 nm, the gallery height roughly corresponds to a double layer of PPA moieties. It should be noted that one hydroxyl group is removed from PPA to make the $[PhPO(OH)O]NbO_5$ environment. In addition, the arrangement of the PPA moieties with respect to the perovskite-like slabs is not clear, and the interlayer distance could be affected by the displacement of two adjacent layers. Thus, no further interpretation of the observed interlayer distance (2.18 nm) is possible.

As regards APA/C_{10}O-HLaNb, a linear relationship is observed between the interlayer distance (after drying, d) and the number of carbon atoms in the *n*-alkyl chain of APA (n_C), as shown in Figure 7

$$d = 0.212n_C + 1.323$$

The increment of the interlayer distance per one carbon atom, 0.212 nm, is larger than the increment for all-trans *n*-alkyl chains (0.127 nm) and smaller than the doubled value (0.254 nm), indicating bilayer arrangement of the *n*-alkyl chains. Because the IR results for C_{18}PA/C_{10}O-HLaNb show that the *n*-$C_{18}H_{37}$ chain has an all-trans conformation and a linear relationship is clearly observed

(61) Gopalakrishnan, J.; Bhat, V.; Raveau, B. *Mater. Res. Bull.* **1987**, *22*, 413–417.

(62) Alberti, G.; Casciola, M.; Costantino, U.; Vivani, R. *Adv. Mater.* **1996**, *8*, 291–303.

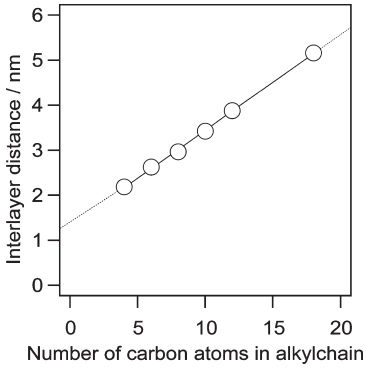

Figure 7. Variation in the interlayer distance of the *n*-alkylphosphonate derivatives of HLaNb (APAs/C_{10}O-HLaNb) after drying at 120 °C as a function of the number of carbon atoms in *n*-alkyl chain.

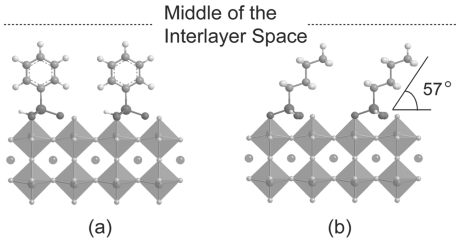

Figure 8. Proposed models for (a) phenylphosphonate derivative of HLaNb (PPA/C_{10}O-HLaNb) and (b) *n*-butylphosphonate derivative of HLaNb (C_4PA/C_{10}O-HLaNb).

in Figure 7, we assume that all the *n*-alkyl chains in APA/C_{10}O-HLaNb exhibit all-trans conformation. Thus, the tilt angle of the *n*-alkyl chains in APA/C_{10}O-HLaNb is estimated to be 57°, which is the same as the tilt angle of *n*-alkoxy derivatives HLaNb[38]. The observed tilt angle (57°) is very close to the value corresponding to the structural model where the P−C bond is perpendicular to the (001) plane. The structural model of C_4PA/C_{10}O-HLaNb is shown in Figure 8, along with the structural model of PPA/C_{10}O-HLaNb.

Conclusions

We have demonstrated that the interlayer surface of $HLaNb_2O_7 \cdot xH_2O$ (HLaNb) can be modified under mild conditions with various organophosphonic acids (phenylphosphonic acid and *n*-alkylphosphonic acids) using the *n*-decoxy derivative of HLaNb (C_{10}O-HLaNb) as an intermediate. The organophosphonic acids [$RPO(OH)_2$] are assumed to be converted into the RPO(OH)(ONb) environment. The successful formation of graft-type organic derivatives (PPA/C_{10}O-HLaNb and APA/C_{10}O-HLaNb) shows that reactions with organophosphonic acids could offer a new approach to the modification of protonated forms of layered oxides. The reaction of *n*-butylamine with PPA/C_{10}O-HLaNb indicates, moreover, that the graft-type organic derivatives obtained in this study can be further utilized as new host compounds in intercalation chemistry.

Acknowledgment. This work was financially supported in part by the Global COE Program "Center for Practical Chemical Wisdom" by MEXT. The authors thank Mr. Yoshitaka Kamochi and Ms. Yumi Kato for their experimental assistance.

Supporting Information Available: Scanning electron micrographs of APAs/C_{10}O-HLaNb (PDF). This material is available free of charge via the Internet at http://pubs.acs.org.